

Research Article

Parameter Sensitivity Analysis of the Hydraulic Fracture Growth Geometry in a Deep Shale Oil Formation: An Experimental Study

Shanzhi Shi,¹ Yushi Zou ,² Lihua Hao,¹ Beibei Chen,¹ Shicheng Zhang,² Xinfang Ma,² and Shipeng Zhang²

¹Engineering Technology Research Institute, PetroChina Xinjiang Oilfield Company, Karamay 834000, China

²State Key Laboratory of Petroleum Resources and Prospecting, China University of Petroleum (Beijing), 102249, China

Correspondence should be addressed to Yushi Zou; zouyushi@126.com

Received 2 April 2022; Revised 19 May 2022; Accepted 2 June 2022; Published 26 June 2022

Academic Editor: Jinze Xu

Copyright © 2022 Shanzhi Shi et al. This is an open access article distributed under the Creative Commons Attribution License, which permits unrestricted use, distribution, and reproduction in any medium, provided the original work is properly cited.

The depth of shale oil of Fengcheng Formation in Mahu of Junggar Basin, China, is 4500–5000 m. The horizontal principal stress difference of deep shale reservoir is high, which makes it difficult to form complex fractures during fracturing reconstruction. In order to fully understand the law of hydraulic fracture propagation in the formation during fracturing construction, the anisotropy characteristics and basic reservoir physical parameters (mineral composition and rock strength parameters) of rock were obtained through mineral composition test and indoor rock mechanics test (Brazil splitting test), and it was found that the heterogeneity was strong. The true triaxial fracturing simulation experimental system is used to carry out experimental research on full-diameter core rock samples, and the propagation patterns of hydraulic fractures under the influence of different geological factors (in situ stress difference and natural fractures) and engineering factors (pumping rate and fracturing fluid viscosity) are compared and analyzed. The results show that the in situ stress is the most important factor affecting fracture propagation, which determines the direction and shape of fracture propagation. The natural weak surface (lamina/bedding and natural fractures, etc.) in shale reservoir is an important reason for complex fractures. The nature of the weak plane, occurrence, and in situ stress jointly determine whether the fracture can extend through the weak plane. With the increase of pumping rate (18 mL/min to 30 mL/min), the ability of hydraulic fractures to penetrate layers is continuously enhanced. The horizontal principal stress difference of deep shale reservoir is high, and the low viscosity fracturing fluid (10 mPa·s) tends to activate the horizontal bedding, while the high viscosity fracturing fluid (80 mPa·s) tends to directly penetrate the bedding to form the vertical main fracture. Therefore, the fracturing technology of alternating injection of prehigh viscosity fracturing fluid and postlow viscosity fracturing fluid can be adopted to maximize the complexity of fracturing fractures in deep shale reservoirs. The research results are designed to provide theoretical guidance for prediction of hydraulic fracturing fracture propagation in shale reservoir and have certain reference significance for field construction.

1. Introduction

Shale oil has become a new hot spot of unconventional oil and gas exploration and development after shale gas [1–3]. China is rich in shale oil resources [1], but most of them need to be effectively developed through large-scale volume transformation [4, 5]. Mahu shale oil is a major exploration area of unconventional oil and gas resources in Junggar Basin. The deep shale reservoir has a large stress difference and it is difficult to form complex fractures [6]. This leads to insufficient volume of res-

ervoir reconstruction [7–11]. In addition, natural fractures, lamina/bedding, and other discontinuous structures in shale have a significant impact on effective reservoir reconstruction volume of hydraulic fracturing. Under high in situ stress difference, effective communication of these discontinuous structural planes during hydraulic fracturing has become the key to the success of deep shale oil reservoir reconstruction. Therefore, the study of fracture propagation characteristics through physical simulation experiment plays an important role in the formulation and implementation of fracturing scheme.

TABLE 1: Comparison of true triaxial hydraulic fracturing experimental fracture monitoring methods.

Monitoring method	Advantages	Disadvantages
Open samples directly [26]	Hydrofracture plane morphology can be directly observed with tracer	It is difficult to obtain three-dimensional fracture morphology of samples; it is difficult to distinguish hydraulic fractures from natural fractures
CT scanning [27]	The distribution of three-dimensional fracture network can be reconstructed without destroying the sample	Poor application effect for large size samples; it is expensive and economical

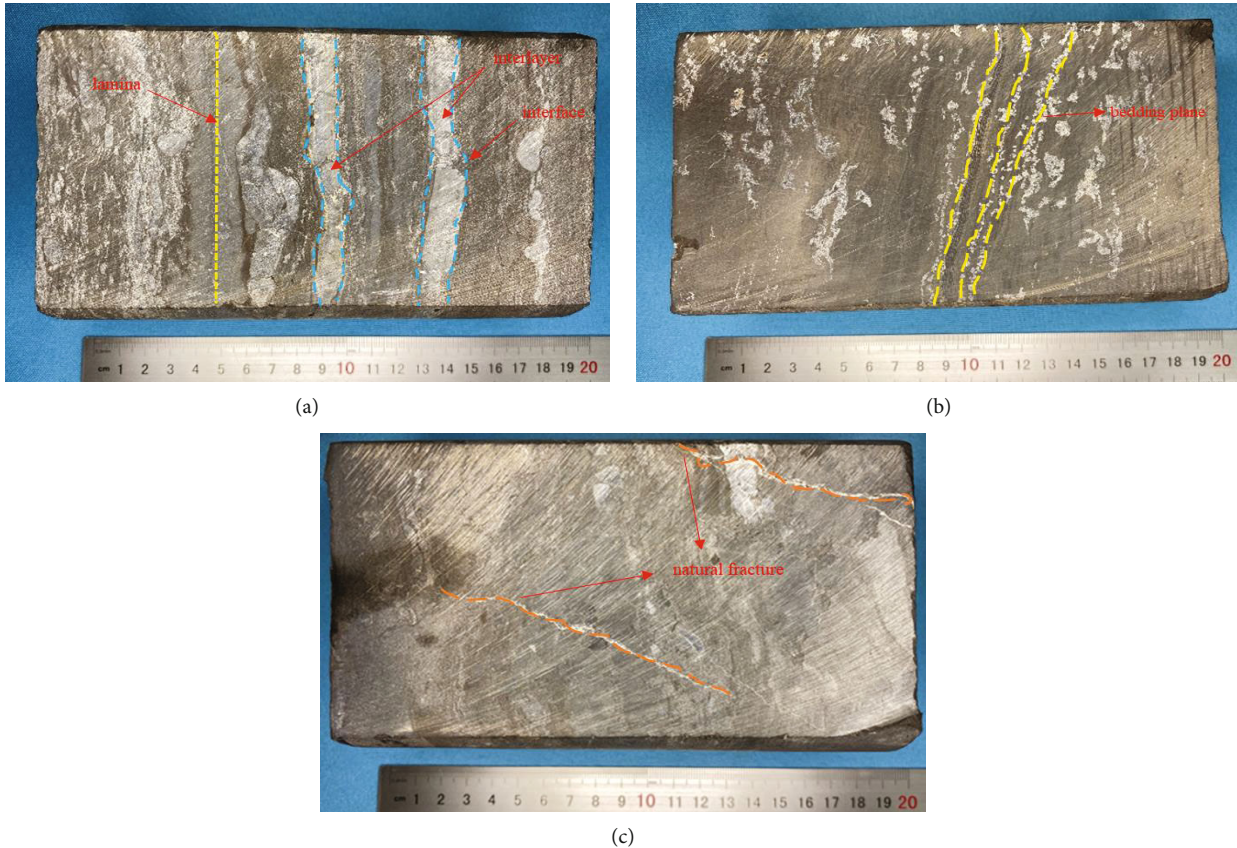
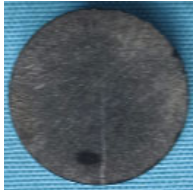
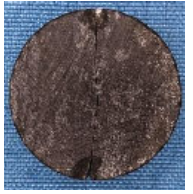




FIGURE 1: Different cores of Permian Fengcheng Formation in Well Maye X1. (a) Core with laminas. (b) Core with beddings. (c) Core with three natural fractures.

Many scholars have studied the fracture propagation law of hydraulic fracturing through experiments. Warpinski and Teufel [12] have proved that geological discontinuities (natural fractures, laminas, bedding planes, etc.) significantly affect the geometric shape of hydraulic fractures, which can restrict the extension of fractures, increase fluid filtration, hinder proppant migration, and increase the possibility of forming complex fractures. Hydraulic fractures tend to penetrate natural fractures when intersecting with a high angle (>45 deg) and tend to be captured or turned when encountering natural fractures with low angle (>45 deg). Blanton [13] summarized the interaction criterion between hydraulic fractures and natural fractures through laboratory tests and theoretical analysis and put forward the conditions for hydraulic fractures to penetrate natural fractures. Xu et al. [14–16] found that different

pore size distributions lead to various transport efficiencies of shale matrix. Effect of nanoscale pore size distribution (PSD) on shale gas production is important. Inject gas can pressurize a thief zone and a less complex and more discrete pore network better benefits the gas injectivity index. Gipson [17] studied the relationship between burial depth, porosity, clay orientation, clay mineral composition, and mineral particle size of the Pennsylvanian shale in western Kentucky and found that with the increase in depth, shale illite content increased and porosity decreased. T. Lo et al. [18] found that shale still has a certain degree of anisotropy under high confining pressure. The factors influencing the fracture height are summarized by Smith et al. [19] as follows: (1) the minimum horizontal principal stress difference between the production layer and the interlayer is the main factor affecting the fracture

TABLE 2: Diagram of experimental fractures in Brazilian splitting.

Core number	Tensile strength (MPa)	Pictures before test	Pictures after test	Fracture morphology of hydraulic fracturing
Parallel to bedding	14.6			The fracture starts and extends along the layer until the sample is completely broken. The propagation path is bedding, and the fracture surface is bedding surface, which is smooth and flat without turning.
Perpendicular to bedding	23			Both the fracture self-loading jaw and the center of the disc can fracture, but the local small-scale bedding fracture around the fracture only occurs when the fracture path is offset. The incomplete penetration of the fracture bedding indicates that the fracture of the bedding is caused by the tensile stress induced by eccentric compression after the fracture of the sample.

height of hydraulic fracturing. (2) The characteristics of the interlayer interface have a great influence on the fracture height of hydraulic fracturing. (3) The difference of rock physical properties and pore pressure in the production interval are the secondary factors affecting the fracture height. (4) Treatment parameters, such as fracturing fluid density and viscosity, proppant concentration, construction pumping rate, and perforation distribution, have great impacts on the geometry of fractures. Through the field and laboratory simulation experiments, the influence of different factors on fracture propagation is analyzed. Sun et al. [20] studied the influence of shale reservoir bedding direction on fracture propagation through large-scale shale hydraulic fracturing simulation test. Shicheng et al. [21] studied hydraulic fracturing fractures of shale outcrop through laboratory fracturing simulation test and found that pumping rate and fracturing fluid viscosity were conducive to the formation of complex fractures within a certain range. When the local stress difference was low, hydraulic fractures were easy to propagate directly along natural fractures. The effect of high local stress difference was favorable for more natural fractures to communicate and form relatively complex fracture network. Kao et al. [22] simulated the fracture propagation of deep shale fracturing and analyzed the morphology of hydraulic fractures under high horizontal stress difference. Xinfang et al. [23] used Longmaxi Formation shale with weak bedding cementation strength to carry out true triaxial fracturing simulation test and found that hydraulic fractures are easy to turn and propagate along the bedding plane, and the vertical propagation of fractures is limited. True triaxial physical simulation experiment is a reliable means to study the law of fracture propagation [24, 25], but the experimental results are not easy to observe, and this problem can be solved by many monitoring methods, as shown in Table 1.

Most of the previous work is aimed at the middle and lower strata (<3500 m), and whether it can strengthen the formation of fracture network under high horizontal stress difference in deep layer remains to be demonstrated. The previous experimental samples mostly used outcrops and concrete, and the experimental simulation was different from the actual

downhole results to some extent [25]. Based on this, a set of small-size true triaxial experiment system was adopted in this paper to conduct fracture propagation simulation experiments on full-diameter core samples with different characteristics. The internal morphology of shale before and after fracturing was observed by CT scanning. The morphology of fracture propagation during hydraulic fracturing in Mahu shale reservoir is discussed.

2. Simulation Test of Hydraulic Fracture Propagation

2.1. Test Basic Physical Parameters. The samples were taken from the full-diameter core of Mahu in the Junggar Basin and from adjacent locations of the same well, as shown in Figure 1. There are no natural fractures in core in Figure 1(a); only thin gray strip interlayers with thickness of 2–3 mm exist. Core in Figure 1(b) has obvious bedding planes and weak interlayer cementation. There is a set of high-angle fractures in core in Figure 1(c) with a width of about 0.5 mm. Before the fracturing experiment, the basic physical parameters such as mineral composition, permeability, and elastic modulus of rock samples were tested.

Mineral composition test results show that the mineral composition of reservoir core presents obvious zoning phenomenon. The main mineral composition are quartz and carbonate; the relative content of which are between 20% and 90%. The clay minerals are mostly less than 10%. After further testing, the clay minerals are mainly composed of two elements, S (smectite) and It (illite). Permeability test results range from 0.06 to $1.05 \times 10^{-3} \mu\text{D}$. It is found that with the increase of depth, the content of clay minerals in the formation gradually decreases, while the content of nonclay minerals gradually increases, but the data fluctuates greatly with the increase of depth without obvious regularity.

The Brazilian test determines the tensile strength of rock by measuring the failure load in the direction of diameter and calculating the size of sample. Brazilian splitting is one of the best methods to analyze the influence of bedding orientation on

fracture propagation under tension. The size of the Brazilian test was 25 mm × 13 mm (diameter × thickness). In the Brazilian test, the open fracture extends perpendicular to the bedding plane, which is similar to the hydraulic fracture propagation model. Table 2 shows two typical fracture morphologies of different bedding orientation in Brazilian test results. The anisotropy of tensile strength is defined as

$$R = \frac{\sigma_{\max}}{\sigma_{\min}}, \quad (1)$$

in which R is the anisotropy of tensile strength, σ_{\max} is the maximum tensile strength, and σ_{\min} is the minimum tensile strength.

The maximum difference of tensile strength is 20 MPa. The anisotropy of elastic modulus is calculated to be 1.7. The reason for the high heterogeneity is that when the bedding angle is small, the shale splits along the bedding direction. At this time, the tensile strength mainly depends on the tensile strength of the weak surface of bedding, so the tensile strength is low. If the bedding angle is 90°, the shale is fractured through the bedding plane. At this time, the tensile strength is influenced by the weak surface of shale and shale matrix, so the tensile strength becomes larger.

2.2. Experimental Device and Sample Preparation. This simulation adopts a set of small-scale true triaxial fracturing simulation experimental system independently developed by the Reservoir Reconstruction Research Office of China University of Petroleum (Beijing) [28]. The system is mainly composed of stress loading system, core chamber, constant speed and constant pressure pump, temperature control system, intermediate container, data acquisition system, auxiliary devices, and other parts [29]. The physical diagram is shown in Figure 2. The three-way stress loading can be stepless adjusted, and the injection pump is a constant speed and pressure pump, which is precisely controlled by a computer to monitor and record the wellhead injection pressure and temperature in real time.

As the cores have been dissected, high strength epoxy resin glue and 20/40 mesh quartz sand was used to fill the missing parts of edges and corners before processing the rock samples, as shown in Figure 3(a). Then, the CNC sand line cutting machine was used to process the rock cubes into 8 cm × 8 cm × 10 cm fracturing samples [30], as shown in Figure 3(b). In the center of the 8 cm × 8 cm cross-section of the rock sample, a drill with an outer diameter of 1.5 cm was used to drill a hole with a depth of 5.3 cm. Finally, the steel pipe (simulated wellbore) with an outer diameter of 1.3 cm, an inner diameter of 0.6 cm, and a length of 5.8 cm was sealed in the hole with high strength epoxy resin glue, and a 1 cm long open hole section was formed at the bottom of the well, as shown in Figure 3(c).

Figure 4 shows the CT scanning results of the open-hole section of the sample, which shows the differences in characteristics of different cores. The experiment was divided into three groups: sample 1# and sample 2#, and sample 3# were used to simulate the influence of weak face on artificial fracture propagation morphology; samples 4# and 5# were used

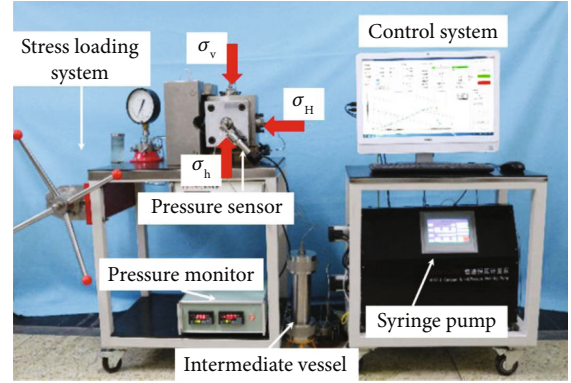


FIGURE 2: Real picture of small size true triaxial fracturing simulation experimental system.

to simulate and analyze the effect of pumping rate on artificial fracture propagation morphology; samples 2# and 6# were used to simulate and analyze the influence of viscosity on artificial fracture propagation morphology. The sampling depth of rock samples is shown in Table 3. The five rock samples are subjected to similar in situ stresses. Therefore, the same stress conditions are used to simulate the experiment. This paper mainly studies the fracture propagation law under deep conditions.

2.3. Experimental Method and Scheme. Due to the limitation of laboratory conditions, it is difficult to obtain the field scale parameters of hydraulic fracturing application. Therefore, according to the performance of laboratory equipment and referring to the theoretical research of Liu et al. [31], the design is based on similarity criteria, including similar energy, similar injection rate, and similar geometric size. In order to meet the conditions, the fracture toughness and permeability of samples need to be very low. At the same time, high viscosity fluid or injection pumping rate should be used to reduce the impact of rock toughness. However, it is difficult to strictly meet this standard in laboratory practice. Therefore, the dimensionless toughness parameter proposed by Savitski and Detournay [32] is used to explain the similarity of fracture propagation. When $\kappa \geq 4$, the hydraulic fracture propagation mode is dominated by rock toughness. When $\kappa \leq 1$, the expansion mode is dominated by viscous dissipation of fracturing fluid flow. When $1 < \kappa < 4$, the extended mode belongs to the transition mode. Field hydraulic fracturing is generally at the viscosity dominated stage. Therefore, in order to reflect the hydraulic fracture propagation under field conditions, reasonable injection parameters (Formula (2)–Formula (5)) are set for indoor experiments: the pumping rate is 18 mL/min (corresponding to pumping rate of 3 m³/min) and 30 mL/min (corresponding to pumping rate of 5 m³/min). There are two kinds of fracturing fluid viscosity: low viscosity (10 mPa·s) fracturing fluid and high viscosity (80 mPa·s) fracturing fluid.

$$\kappa = K' \left(\frac{t^2}{\mu' 5Q^3 E' 13} \right)^{1/18}, \quad (2)$$

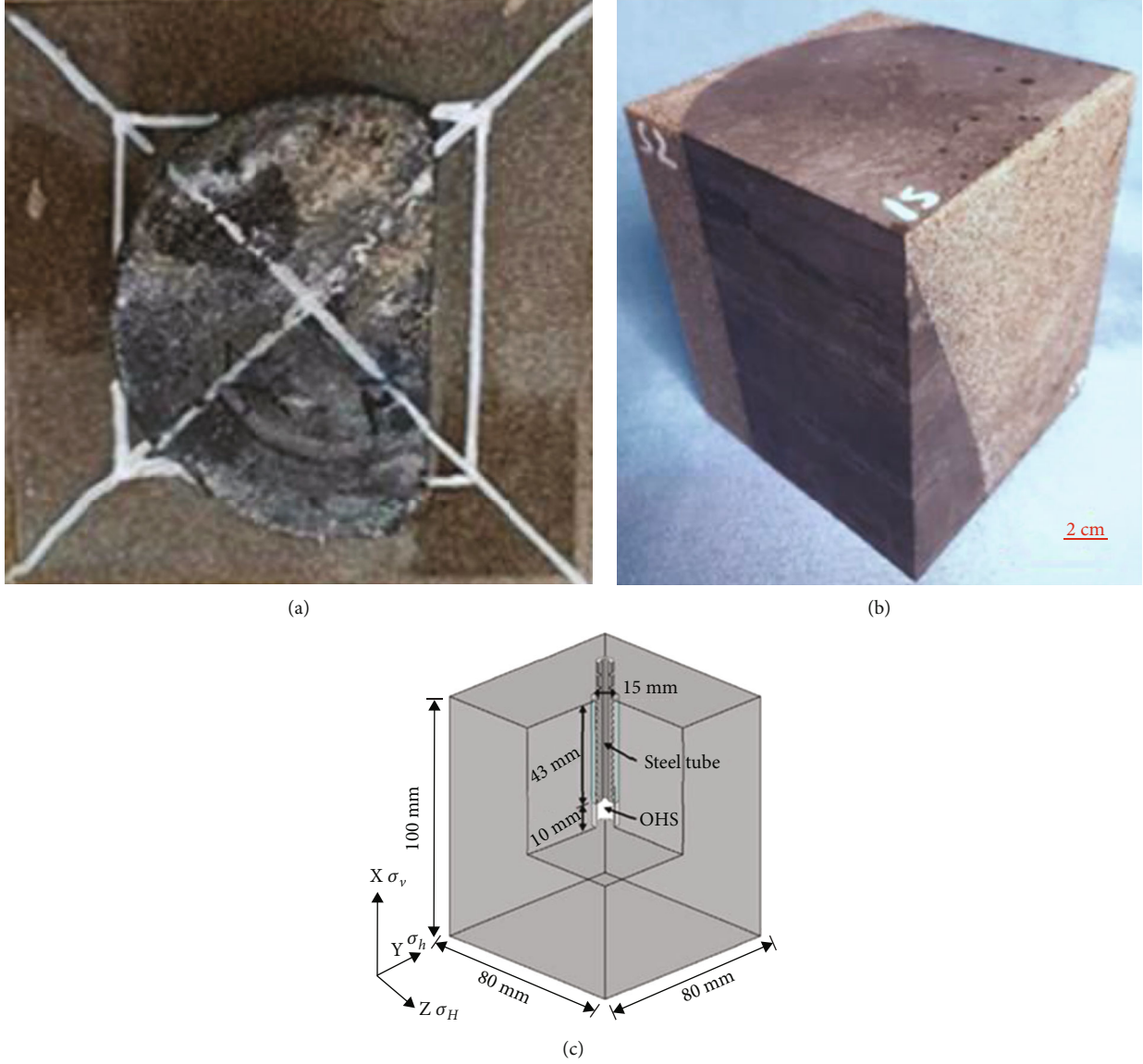


FIGURE 3: Schematic diagram of full diameter core and physical model sample and well completion. (a) Core sizing and setting process. (b) Fracturing test sample. (c) Schematic diagram of well completion.

$$K' = 4 \left(\frac{2}{\pi} \right)^{1/2} K_{IC}, \quad (3)$$

$$E' = \frac{E}{1 - \nu^2}, \quad (4)$$

$$\mu' = 12\mu, \quad (5)$$

in which κ is the dimensionless toughness parameter ($\text{Pa}\cdot\text{m}^{1/2}$), Q is pumping rate (mL/min) K_{IC} is the fracture toughness of the rock ($\text{Pa}\cdot\text{m}^{1/2}$), E is Young's modulus (Pa), ν is Poisson's ratio, μ is fracturing fluid viscosity ($\text{Pa}\cdot\text{s}$), K' is the material parameter ($\text{Pa}\cdot\text{m}^{1/2}$), E' is the material parameter (Pa), and μ' is the material parameter ($\text{Pa}\cdot\text{s}$).

To simulate the triaxial stress states of the well, the horizontal minimum horizontal stress (σ_h), horizontal maximum horizontal stress (σ_H), and vertical stress (σ_v) were applied using triaxial hydraulic loading, as shown in Figure 3(c). The wellbore direction is consistent with the vertical stress (σ_v). The triaxial stress is maintained by a hydraulic servo system. The stress mechanism of Mahu is simulated, and the horizontal stress difference was kept at 25 MPa.

In order to facilitate the observation of the hydraulic fracture morphology, fracturing simulation experiments were carried out in the fracturing fluid mixed with fluorescent agent. After the test, the morphology of hydraulic fractures was determined according to the distribution of staining fluid on the surface and inside the sample. In the process of fracturing simulation, the intermediate container pipeline of fracturing fluid is

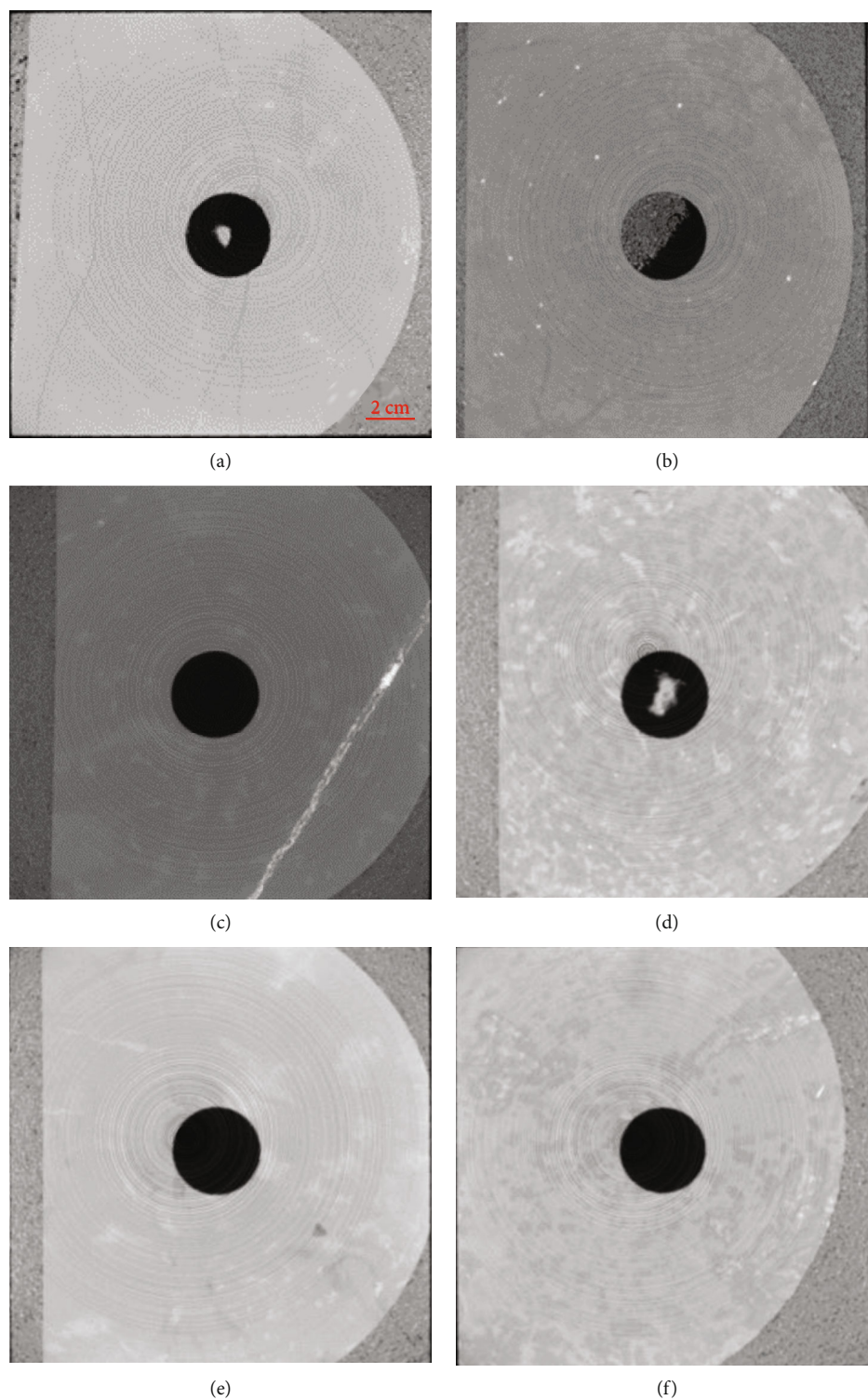


FIGURE 4: CT scan of open-hole. (a) Sample 1#. (b) Sample 2#. (c) Sample 3#. (d) Sample 4#. (e) Sample 5#. (f) Sample 6#.

TABLE 3: Depth of experimental sample.

Number	Sample 1#	Sample 2#	Sample 3#	Sample 4#	Sample 5#	Sample 6#
Depth (m)	4562.9	4556.8	4558.8	4531.6	4571.8	4554.2

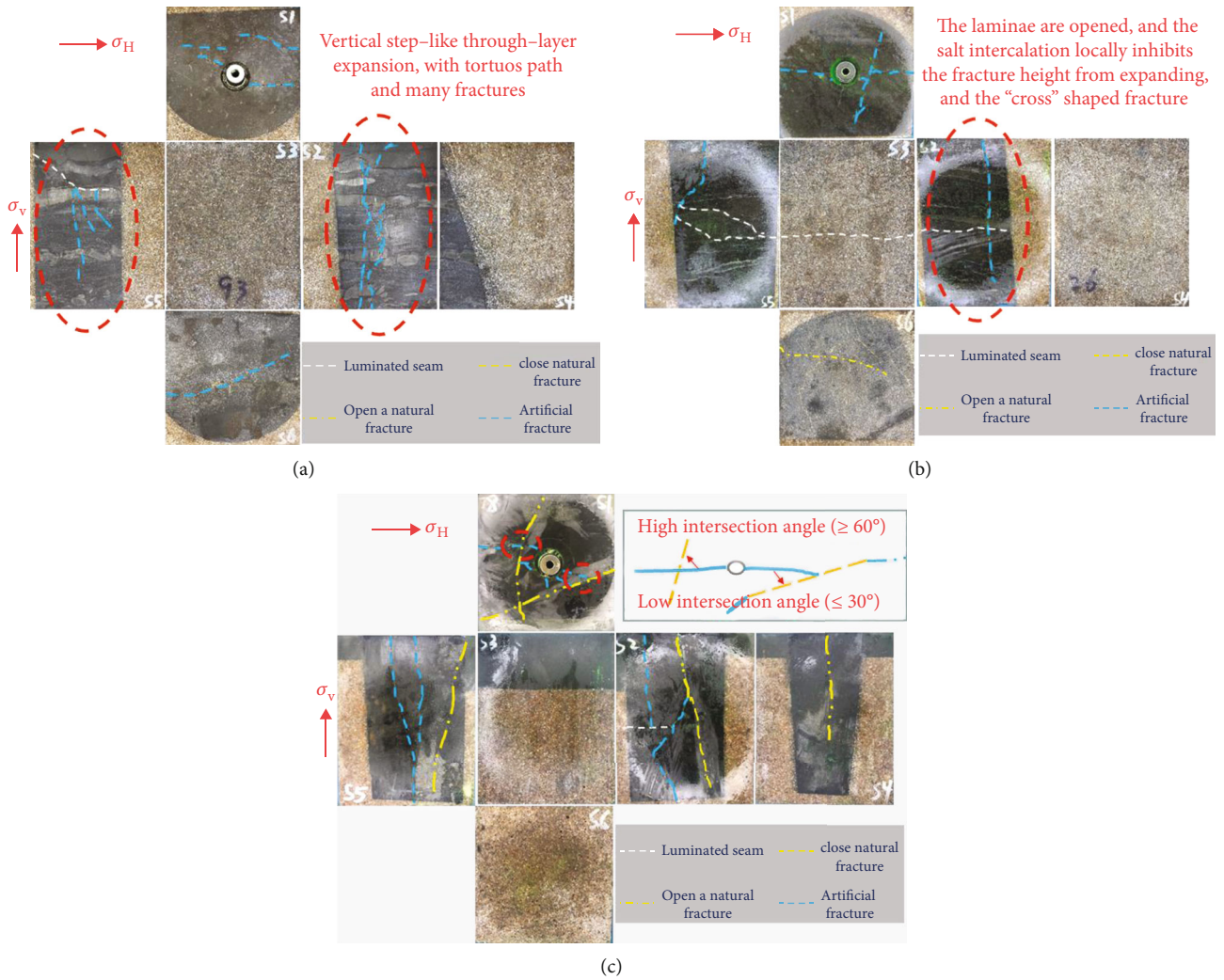


FIGURE 5: Fracture morphology of sample surface after fracturing. (a) Sample 1#. (b) Sample 2#. (c) Sample 3#.

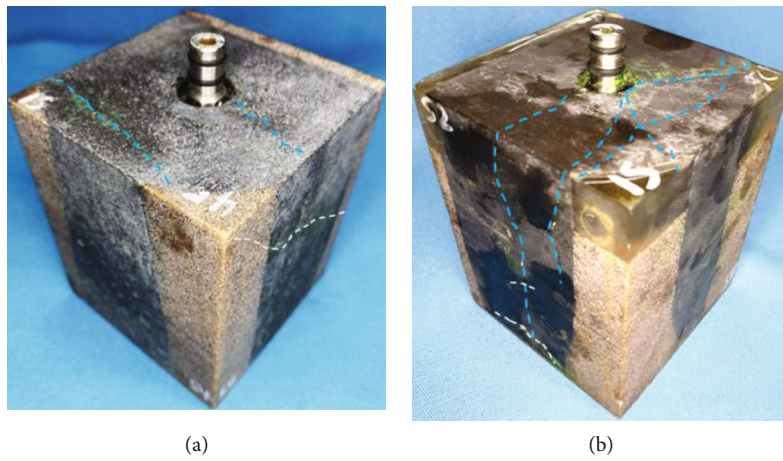


FIGURE 6: Diagram of sample after fracturing. (a) Sample 4#. (b) Sample 5#.

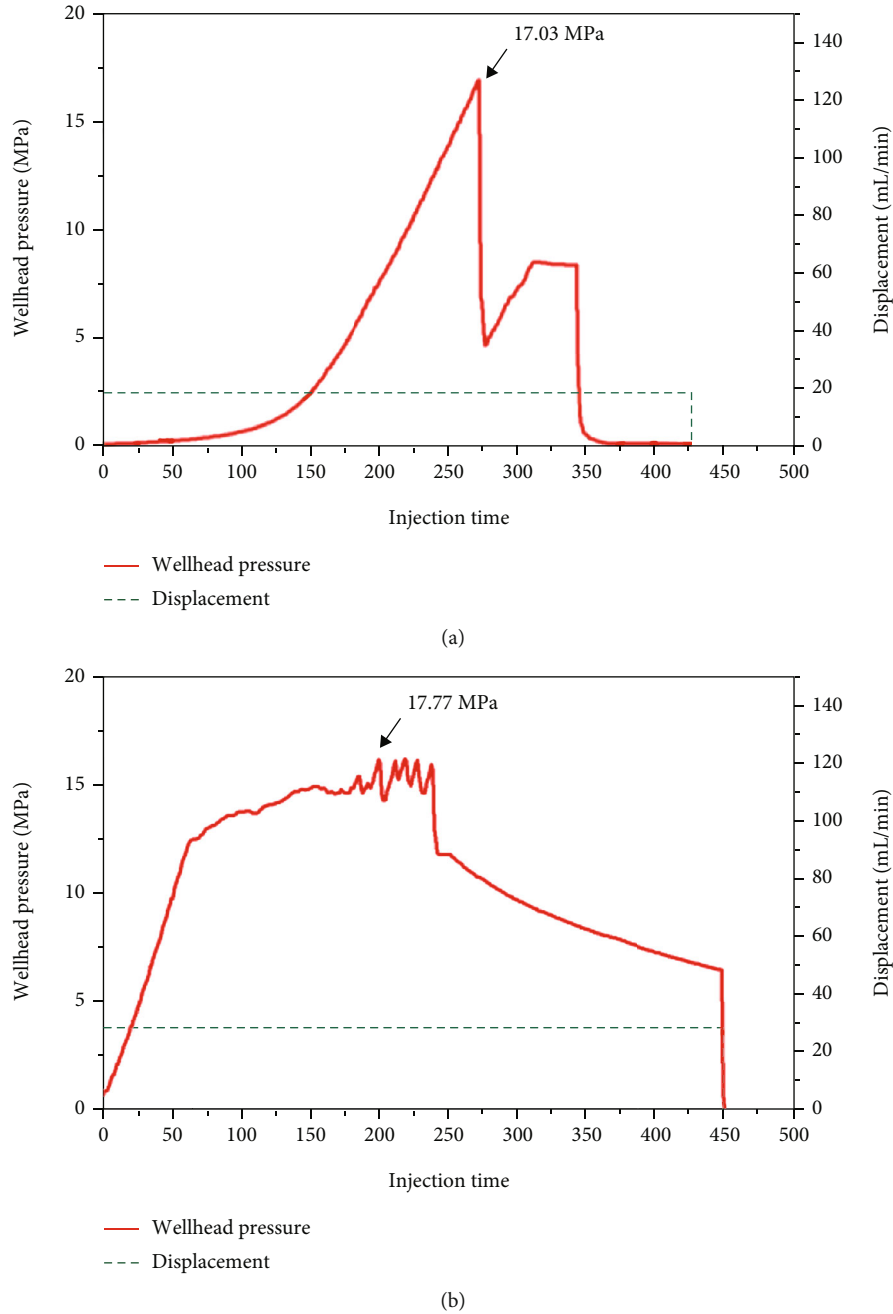


FIGURE 7: Injection pressure curve of different pumping rates. (a) Sample 4#. (b) Sample 5#.

connected to the wellhead, and the fracturing fluid in the intermediate vessel is injected into the wellbore at a constant rate with a constant speed pump, and the pressure sensor at the wellhead synchronously collects pressure changes throughout the fracturing process. When the wellhead pressure drops rapidly and no longer increases, the pump stops. After the experiment, the rock samples were taken out from the sample chamber, and the fracture morphology and proppant distribution of the rock samples were identified through comprehensive analysis of CT scanning, tracer distribution, and rock sample division [27]. And the fracture propagation characteristics were analyzed based on the injection pressure curve.

3. Experimental Results and Analysis

3.1. Effect of Bedding/Lamination/Natural Fracture on Fracture Morphology. Three groups of horizontal well fracturing experiments with different development characteristics were carried out according to the experimental scheme. The fracture morphology results are shown in Figure 5, in which the blue dotted lines are artificial fractures, the white dotted lines are lamination/bedding, and the yellow dotted lines are natural fractures.

The results show that there are three typical experimental patterns of vertical fracture extension under the action of

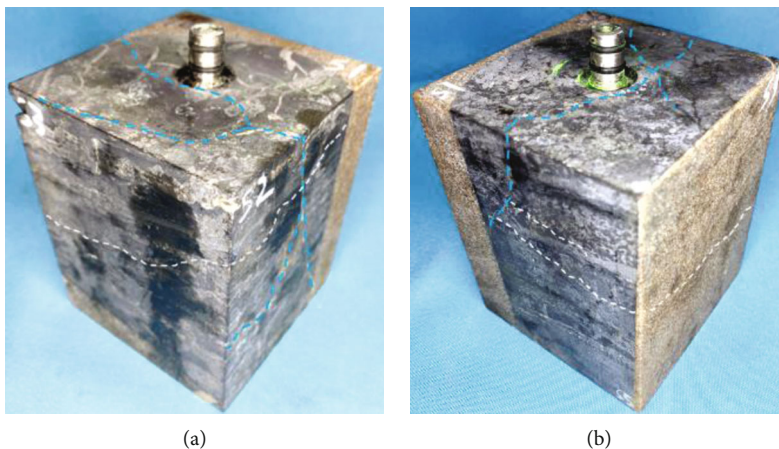


FIGURE 8: Diagram of sample after fracturing. (a) Sample 6#. (b) Sample 2#.

stratification: directly through the stratification, trapped by stratification, and migration. When the fracture is orthogonal to bedding, the difference in the cementation strength of bedding plane will lead to different propagation patterns of the fracture: there are two striped layers in 1# (Figure 5(a)), with strong cementation strength. The hydraulic fracture starts along the direction of maximum horizontal principal stress and turns through the two striped layers in longitudinal expansion, with tortuous paths and multiple fractures. The horizontal bedding is obvious in the 2# dark gray shale, and the cementation strength is weak. The hydraulic fractures start along the direction of the maximum horizontal principal stress and are captured by the horizontal bedding after longitudinal penetration, resulting in shear or opening of the horizontal bedding. The longitudinal extension of hydraulic fractures in the 2# shale is obviously limited by bedding.

Under the condition of certain approaching angle and horizontal principal stress difference, natural fracture will change the extension form of hydraulic fracture [33, 34]. When the approach angle is larger than 60° and the stress difference is higher, hydrofractures tend to continue to extend through natural fractures. When the approach angle is small (less than 30°) and the stress difference is low, the hydraulic fracture tends to turn to continue to extend along the natural fracture. In other cases, when hydraulic fractures intersect with natural fractures, they are often accompanied by mixed extension of crossing, opening, and branching [4, 5]. There is a group of calcite filled natural fractures developed in 3# grey siltstone. Fracturing fluid is lost along low angle fractures, leading to local diversion of artificial fractures, and hydraulic fractures spread through high angle fractures.

It can be seen that weak surface can increase the fracture density of hydraulic fracturing, thus improving the adequacy and stimulation effect of reservoir stimulation. However, the opening of too many bedding will restrict the expansion of hydraulic fractures in the length and height direction and reduce the volume of effective reservoir reconstruction.

3.2. Effect of Pumping Rate on Fracture Propagation Morphology. Pumping rate is one of the important engineering factors affecting fracturing effect [35, 36]. It is of great signifi-

cance to study the influence of pumping rate on hydraulic fracture propagation in Mahu deep tight shale reservoir. Sample 4# and sample 5# are subject to hydraulic fracturing test with pumping rate of 18 mL/min and 30 mL/min, respectively. Both 4# and 5# have similar development characteristics. The sample after fracturing is shown in Figure 6, and the pumping pressure curve is shown in Figure 7.

In the process of 4# flow rate (18 mL/min) fracturing, the pressure rises gradually. When it reaches 17.03 MPa (250 s), the sample cracks and forms a fracture, and then, the pressure drops rapidly. With the injection of fracturing fluid, the bottom hole pressure continues to rise slowly and fluctuates slightly, indicating that the fracture communicates with the weak side during the expansion process. After the bottom hole pressure reaches about 8.5 MPa, the pressure will not rise for a period of time and the pump will be stopped. In the process of 5# flow rate (30 mL/min) fracturing, the sample starts to crack when the bottom hole pressure reaches 12.99 MPa (70 s). With the injection of fracturing fluid, the bottom hole pressure continues to rise slowly and then cracks again when the maximum pressure reaches 17.77 MPa. After that, four small spikes appear in the pressure fluctuation, forming multiple branch fractures. Then, the pressure drops to 12 MPa, the pump is stopped, the bottom hole pressure decreases, and the fracturing fluid flows to the sample surface through the formed hydraulic fractures. After fracturing, the fractures are complicated. Increasing pumping rate can communicate more weak points, thus increasing effective stimulated reservoir volume (ESRV).

3.3. Influence of Fracturing Fluid Viscosity on Fracture Propagation Morphology. Fracturing fluid performance mainly includes friction characteristics, rheological characteristics, and filtration performance, while viscosity can be used as a comprehensive index [37]. The change of fracturing fluid viscosity can affect the performance of fracturing fluid such as friction, sand suspension, filtration, and flowback. Fracture morphology and pressure curves of samples 6# and 2# are shown in Figures 8 and 9. Fracturing fluid viscous (80 mPa·s) under the condition of sample 6# pressurization rate quickly, the formation of fracture width is bigger, the fracture pressure

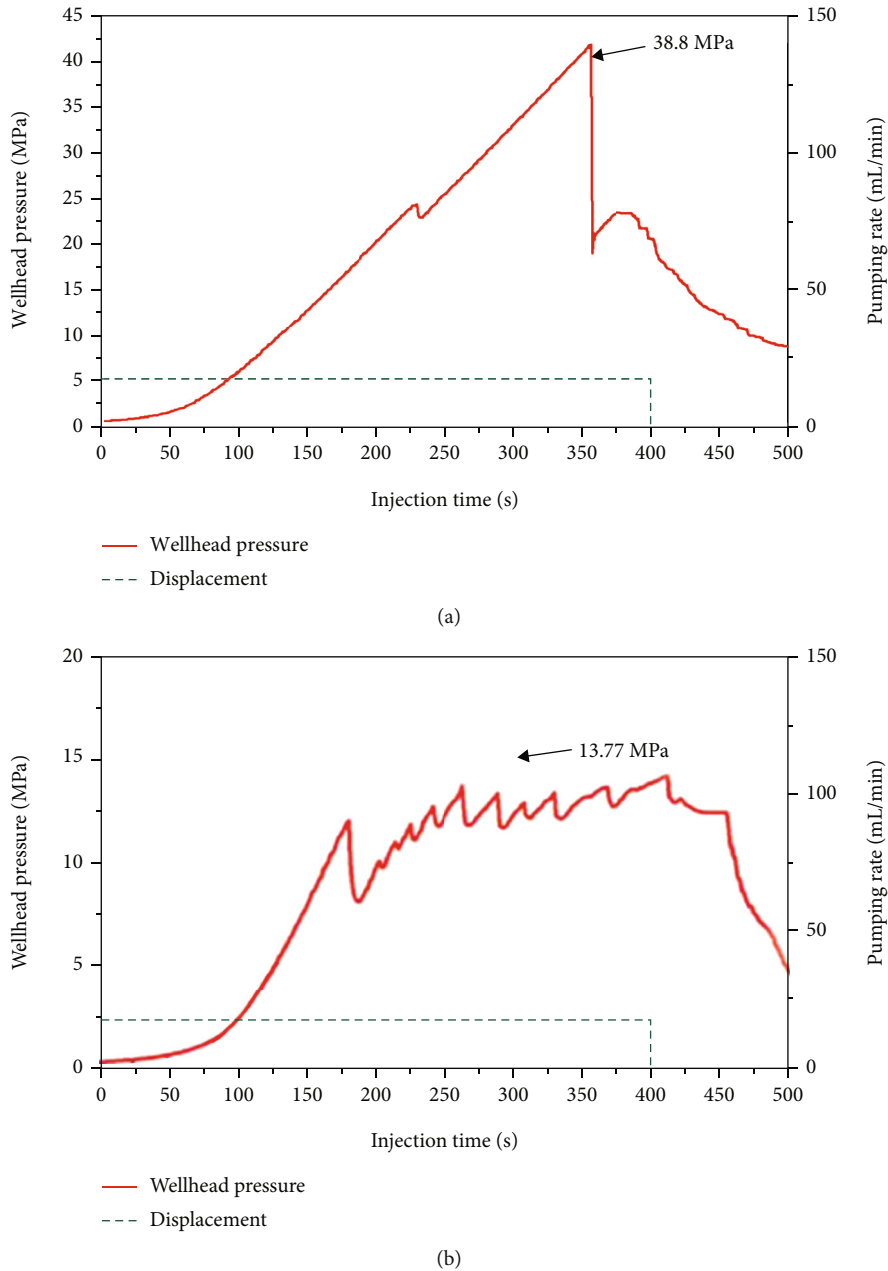


FIGURE 9: Injection pressure curve of different pumping rate pumps. (a) Sample 6#. (b) Sample 2#.

is 38.8 MPa, midway through a rush that accompany branch seam formation, longitudinal extension on full hydraulic fracture after fracturing, the bonding interface, hydraulic fracture directly through the vertical stratification, seam fractures formed near the bedding branch at the same time. It shows that the fracturing fluid is less filtrated into the bedding. Under the condition of low viscosity of fracturing fluid (10 mPa·s), sample 2# was not completely fractured, with continuous high pressure and narrow and tortuous fracture width. The fracture pressure of the sample was 13.7 MPa, which decreased by 65% compared with the hydraulic fracture of high viscosity fracturing. A longi-

tudinal hydraulic fracture was formed, which was only 4.3 cm in height. The fracture fluid filtration is large, and the filtration fluid has a certain lubrication effect, which reduces the shear strength of weak interlayer surfaces, and leads to activation of weak interlayer surfaces connected with vertical main hydraulic fractures, forming complex hydraulic fracture networks.

For the deep shale reservoir with high ground stress difference and well-developed bedding, it is suggested that the fracturing fluid with high viscosity should be used first to form the main fractures to break through the bedding interference near the wellbore and then injected into low seam fracturing fluid

viscosity activation and the main interaction of bedding, with increasing the complexity of fractures, as much as possible to help maximize shale reservoir modification effect.

4. Conclusions

In this paper, an indoor fracturing simulation experiment was carried out on full-diameter tight shale core samples of Mahu to study and the influence of different factors on fracture propagation in this area. After the study, the following conclusions are drawn:

- (a) Laminae, bedding, or millimeter-scale lithological interbeds (dolomite, quartz, and salt) can be opened, locally inhibiting the seam height extension and the overall penetration of layers. Whether the natural fracture is opened or not is affected by many factors such as cementation strength and permeability, and there is uncertainty
- (b) The high pumping rate (30 mL/min) is conducive to the fracture height passing through laminar and lithologic interlayer and opening natural fractures locally. Under the effect of the stress difference in the reservoir, when the pumping rate is high, the fractures can penetrate into the reservoir more quickly and expand rapidly in the reservoir. When the pumping rate is low, the fracture expands slowly and has little influence on fracture propagation morphology
- (c) Viscosity of fracturing fluid has a more significant effect on fracture expansion. The high viscosity (80 mPa·s) fracturing fluid is conducive to increasing fracture pressure and facilitating artificial fractures through laminae and bedding. Under the condition of 25 MPa horizontal stress difference, the fracture width formed by low viscosity fracturing fluid (10 mPa·s) is narrow and tortuous compared with high viscosity fracturing fluid. It is recommended to use high viscosity fracturing fluid as front fluid

Data Availability

The data used to support the findings of this study are available from the corresponding author upon request.

Conflicts of Interest

The authors declare that there is no conflict of interest regarding the publication of this paper.

Authors' Contributions

Conceptualization and methodology were performed by Shanzhi Shi and Yushi Zou; formal analysis was performed by Shipeng Zhang and Lihua Hao; investigation was carried out by Lihua Hao and Beibei Chen; resources were provided by Shicheng Zhang and Xinfang Ma; writing the original draft preparation was performed by Shipeng Zhang; writing, reviewing, and editing were the responsibility of Yushi Zou; visualiza-

tion was carried out by Yushi Zou and Shipeng Zhang; supervision was performed by Shicheng Zhang and Xinfang Ma; project administration was contributed by Shanzhi Shi, Lihua Hao, and Beibei Chen. All authors have read and agreed to the published version of the manuscript.

Acknowledgments

This study was supported by the National Natural Science Foundation of China (51974332).

References

- [1] Z. Caineng, Y. Zhi, C. Jingwei et al., "Formation mechanism, geological characteristics and development strategy of non-marine shale oil in China," *Petroleum Exploration and Development*, vol. 40, no. 1, pp. 15–27, 2013.
- [2] Y. A. N. G. Zhi, H. O. U. Lianhua, T. A. O. Shizhen et al., "Formation and "sweet area" evaluation of liquid-rich hydrocarbons in shale strata," *Petroleum Exploration and Development*, vol. 42, no. 5, pp. 609–620, 2015.
- [3] Z. H. A. O. Wenzhi, H. U. Suyun, H. O. U. Lianhua et al., "Types and resource potential of continental shale oil in China and its boundary with tight oil," *Petroleum Exploration and Development*, vol. 47, no. 1, pp. 1–11, 2020.
- [4] J. Chengzao, Z. Min, and Z. Yongfeng, "Unconventional hydrocarbon resources in China and the prospect of exploration and development," *Petroleum Exploration and Development*, vol. 39, no. 2, pp. 139–146, 2012.
- [5] W. Qi, X. Yun, W. Xiaoquan, W. Tengfei, and S. Zhang, "Volume fracturing technology of unconventional reservoirs: connotation, optimization design and implementation," *Petroleum Exploration and Development*, vol. 39, no. 3, pp. 252–258, 2012.
- [6] M. J. Mayerhofer, E. Lolon, N. R. Warpinski, C. L. L. Cipolla, D. Walser, and C. M. M. Rightmire, "What is stimulated reservoir volume?," *SPE Production & Operations*, vol. 25, no. 1, pp. 89–98, 2010.
- [7] L. Pan, H. Wang, J. He, F. Li, T. Zhou, and X. Li, "Progress of simulation study on the migration and distribution of proppants in hydraulic fractures," *Natural Gas Industry*, vol. 40, no. 10, pp. 54–65, 2020.
- [8] J. C. Guo, Z. H. Zhao, Q. Lu, C. Yin, and C. Chen, "Research progress in key mechanical theories of deep shale network fracturing," *Natural Gas Industry*, vol. 41, no. 1, pp. 102–117, 2021.
- [9] S. Heng, C. H. Yang, Y. J. Zeng, Y. T. Guo, L. Wang, and Z. K. Hou, "Experimental study on hydraulic fracture geometry of shale," *Chinese Journal of Geotechnical Engineering*, vol. 36, no. 7, pp. 1243–1251, 2014.
- [10] H. O. U. Bing, C. H. E. N. Mian, L. I. Zhimeng, W. A. N. G. Yonghui, and D. I. A. O. Ce, "Propagation area evaluation of hydraulic fracture networks in shale gas reservoirs," *Petroleum Exploration and Development*, vol. 41, no. 6, pp. 833–838, 2014.
- [11] M. Li, F. Zhou, L. Yuan et al., "Numerical modeling of multiple fractures competition propagation in the heterogeneous layered formation," *Energy Reports*, vol. 7, pp. 3737–3749, 2021.
- [12] N. R. Warpinski and L. W. Teufel, "Influence of geologic discontinuities on hydraulic fracture propagation," *Journal of Petroleum Technology*, vol. 24, no. 4, p. 134, 1984.

- [13] T. L. Blanton, "An experimental study of interaction between hydraulically induced and pre-existing fractures," *SPE Unconventional Gas Recovery Symposium*, p. 10847, 1982.
- [14] J. Xu, K. Wu, R. Li et al., "Real gas transport in shale matrix with fractal structures," *Fuel*, vol. 219, pp. 353–363, 2018.
- [15] J. Xu, K. Wu, R. Li et al., "Nano-scale pore size distribution effects on gas production from fractal shale rocks," *Fractals*, vol. 27, no. 8, p. 1950142, 2019.
- [16] X. U. Jinze, C. H. E. N. Zhangxin, and L. I. Ran, "Impacts of pore size distribution on gas injection in intraformational water zones in oil sands reservoirs," *Oil & Gas Science and Technology*, vol. 75, no. 6, p. 75, 2020.
- [17] M. Gipson, "A study of the relations of depth, porosity and clay mineral orientation in Pennsylvanian shales," *Journal of Sedimentary Research*, vol. 36, no. 4, pp. 888–903, 1966.
- [18] T.-w. Lo, K. B. Coyner, and M. N. Toksöz, "Experimental determination of elastic anisotropy of Berea sandstone, Chicopee shale and Chelmsford granite," *Geophysics*, vol. 51, no. 1, pp. 164–171, 1986.
- [19] M. B. Smith, A. B. Bale, L. K. Britt, H. H. Klein, E. Siebrits, and X. Dang, "Layered modulus effects on fracture propagation," in *SPE annual technical conference and exhibition*, New Orleans, Louisiana, October 2001.
- [20] S. U. N. Keming, Z. H. A. N. G. Shucui, and X. I. N. Liwei, "Impacts of bedding directions of shale gas reservoirs on hydraulically induced crack propagation," *Natural Gas Industry*, vol. 3, no. 2, pp. 139–145, 2016.
- [21] Z. H. A. N. G. Shicheng, G. U. O. Tiankui, Z. H. O. U. Tong, Z. Yushi, and M. Songru, "Fracture propagation mechanism experiment of hydraulic fracturing in natural shale," *Acta Petrolei Sinica*, vol. 35, no. 3, p. 496, 2014.
- [22] J. W. Kao, Y. Jin, W. N. Fu et al., "Experimental research on the morphology of hydraulic fractures in deep shale under high difference of in-situ horizontal stresses," *Chinese Journal of Rock Mechanics and Engineering*, vol. 37, no. 6, pp. 1332–1339, 2018.
- [23] M. A. Xinfang, L. I. Ning, Y. I. N. Congbin et al., "Hydraulic fracture propagation geometry and acoustic emission interpretation: a case study of Silurian Longmaxi Formation shale in Sichuan Basin, SW China," *Petroleum Exploration and Development*, vol. 44, no. 6, pp. 1030–1037, 2017.
- [24] Z. O. U. Yushi, M. A. Xinfang, Z. H. O. U. Tong et al., "Hydraulic fracture growth in a layered formation based on fracturing experiments and discrete element modeling," *Rock Mechanics and Rock Engineering*, vol. 50, no. 9, pp. 2381–2395, 2017.
- [25] L. I. U. Naizhen, Z. Zhang, Z. O. U. Yushi, M. A. Xinfang, and Y. Zhang, "Propagation law of hydraulic fractures during multi-staged horizontal well fracturing in a tight reservoir," *Petroleum Exploration and Development*, vol. 45, no. 6, pp. 1129–1138, 2018.
- [26] G. Zhang, D. W. Zhou, J. M. Dou, Y. Nie, and H. Dong, "Experiments on hydraulic fracture propagation under action of natural fractures and crustal stress difference," *Journal of China University of Petroleum*, vol. 43, no. 5, pp. 157–162, 2019.
- [27] Z. Yushi, Z. Shicheng, Z. Tong, Z. Xiang, and G. Tiankui, "Experimental investigation into hydraulic fracture network propagation in gas shales using CT scanning technology," *Rock Mechanics and Rock Engineering*, vol. 49, no. 1, pp. 33–45, 2016.
- [28] Y. Zou, N. Li, X. Ma, S. Zhang, and S. Li, "Experimental study on the growth behavior of supercritical CO₂-induced fractures in a layered tight sandstone formation," *Journal of Natural Gas Science and Engineering*, vol. 49, pp. 145–156, 2018.
- [29] S. Li, X. Ma, S. Zhang, Y. Zou, N. Li, and Z. Zhang, "Experimental investigation on the influence of CO₂-brine-rock interaction on tight sandstone properties and fracture propagation," *Xinjiang Petroleum Geology*, vol. 40, no. 3, pp. 312–318, 2019.
- [30] Z. O. U. Yushi, S. H. I. Shanzhi, S. Zhang et al., "Experimental modeling of sanding fracturing and conductivity of propped fractures in conglomerate: a case study of tight conglomerate of Mahu sag in Junggar Basin, NW China," *Petroleum Exploration and Development*, vol. 48, no. 6, pp. 1383–1392, 2021.
- [31] G. H. Liu, F. Pang, and Z. X. Chen, "Development of scaling laws for hydraulic fracture simulation tests," *Journal of China University of Petroleum*, vol. 5, pp. 45–48, 2000.
- [32] A. Savitski and E. Detournay, "Solution auto-semblable d'une fracture hydraulique ciculaire se propageant dans un milieu elastique sans tenacite," *Comptes Rendus de l'Academie des Sciences Series IIB Mechanics*, vol. 329, no. 4, pp. 255–262, 2001.
- [33] Z. O. U. Yushi, Z. H. A. N. G. Shicheng, Z. H. O. U. Tong, Z. Xiang, and G. Tiankui, "Experimental investigation into hydraulic fracture network propagation in gas shales using CT scanning technology," *Rock Mechanics and Rock Engineering*, vol. 49, no. 1, pp. 33–45, 2016.
- [34] Z. Jian, "Experimental study on hydraulic fracture initiation and propagation in naturally fractured reservoirs," *China University of Petroleum, Beijing*, vol. 5, pp. 109–113, 2007.
- [35] X. Hui, "Research of hydraulic fracturing dynamic propagation in naturally fractured reservoirs," *Southwest Petroleum University*, 2014.
- [36] W. Kan and J. E. Olson, "Mechanics analysis of interaction between hydraulic and natural fractures in shale reservoirs," in *Unconventional Resources Technology Conference*, Denver, Colorado, August 2014.
- [37] Y. Zeng, J. Zhou, H. Wang et al., "Physical simulation of true triaxial variable displacement hydraulic fracturing in deep shale," *Journal of Rock Mechanics and Engineering*, vol. 38, no. 9, pp. 1758–1766, 2019.
- [38] G. Dwivedi and M. P. Sharma, "Application of Box-Behnken design in optimization of biodiesel yield from Pongamia oil and its stability analysis," *Fuel*, vol. 145, pp. 256–262, 2015.